2014-01-1101
Published 04/01/2014

doi:10.4271/2014-01-1101
saeeng.saejournals.org

Modeling Internal Combustion Engine with Thermo-Chemical Recuperation of the Waste Heat by Methanol Steam Reforming

Arnon Poran, Moris Artoul, Moshe Sheintuch, and Leonid Tartakovsky
Technion Israel Inst. of Technology

ABSTRACT

This paper describes a model for the simulation of the joint operation of internal combustion engine (ICE) with methanol reformer when the ICE is fed by the methanol steam reforming (SRM) products and the energy of the exhaust gases is utilized to sustain endothermic SRM reactions. This approach enables ICE feeding by a gaseous fuel with very favorable properties, thus leading to increase in the overall energy efficiency of the vehicle and emissions reduction.

Previous modeling attempts were focused either on the performance of ICE fueled with SRM products or on the reforming process simulation and reactor design. It is clear that the engine performance is affected by the composition of the reforming products and the reforming products are affected by the exhaust gas temperature, composition and flow rate. Due to the tight interrelations between the two main parts of the considered ICE-reformer system, it is desirable to create a single model that simulates joint operation of the ICE and the SRM reactor. Such a model is built with the GT-Power software. It employs published catalytic reactions kinetics. The reformer model is validated using experimental results from a small scale model reactor.

The developed model can be used for the performance optimization of the whole ICE - reformer system including design of the reactor. Simulations with a reformer bed geometry of counter current, multiple tubes performed using the developed model show that heat-transfer is limiting the reformer size, requiring 1.5 m^2 for complete methanol conversion in lean operation of a 75 kW ICE. Moreover the model can be applied to predict a transient behavior of the system owing to the time dependent approach implemented in the reformer and engine calculations.

CITATION: Poran, A., Artoul, M., Sheintuch, M., and Tartakovsky, L., "Modeling Internal Combustion Engine with Thermo-Chemical Recuperation of the Waste Heat by Methanol Steam Reforming," *SAE Int. J. Engines* 7(1):2014, doi:10.4271/2014-01-1101.

INTRODUCTION

Internal combustion engine is the main power plant in most of the modern transportation systems. As such, it is responsible for a substantial part of petroleum fuel consumption as well as environmental pollution. This fact together with a need for a dramatic greenhouse gas emissions reduction provides a powerful incentive to design energy efficient vehicles operated with alternative fuels. This approach can reduce the economic dependence on expensive oil, contribute significantly to climate change mitigation and decrease the global pollution [1].

Since about 30% of the fuel's energy is wasted along with the hot exhaust gases, utilizing a part of this energy is one of the promising methods of engine efficiency improvement. The most common way of waste heat recovery is turbo-charging. Another way - is by using the energy of exhaust gases to promote endothermic reactions of fuel reforming. This method is frequently called thermo-chemical recuperation (TCR) [2]. TCR can be more profitable than turbo-charging because its energy transfer is not bounded by isentropic expansion. The idea of TCR through methanol decomposition or reforming is not new and has been investigated in the last few decades. Pettersson et al [3] summed most of the research conducted up to the early 90's. Finegold et al [4] and Takayuki et al [5] had even built cars with on-board methanol decomposition reporting up to 40% increase in efficiency compared to a same type gasoline operated vehicle. Brinkman and Stebar [6] pointed out that a major contribution to the efficiency increase is due to the favorable properties of the decomposition products such as higher flame speed and octane number, wider flammability limits etc. compared to gasoline. The main problems reported in these preceding studies are backfire, coke formation on the reformer, cold start difficulties, lower maximum power due to reduced air charging, formaldehyde formation (in the cases of liquid methanol burning) and pre-ignition.

Research groups from MIT, AVL and MONSANTO [7, 8, 9, 10] overcame some of these drawbacks by feeding the ICE with low temperature ethanol reformate consisted of equal molar fractions of hydrogen, CO and methane. Their studies show brake thermal efficiency (BTE) improvement of 10-17% and 20-25% compared to an ICE fed with E85 and gasoline, respectively. Tartakovsky et al [11, 12] proposed a hybrid direct injection (DI) ICE-methanol steam reforming system (shown in fig. 1) as another way of solving these problems. The paper explores this scheme.

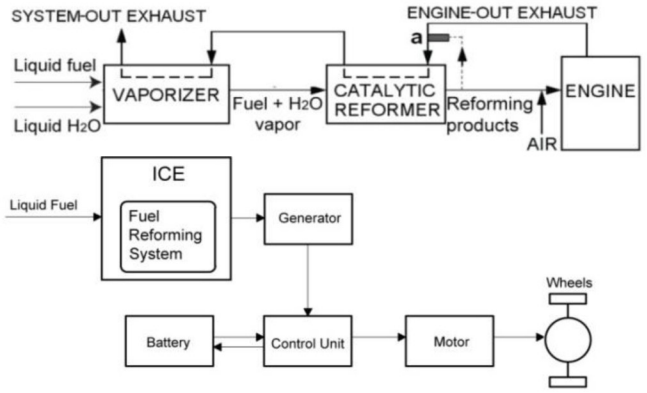

Figure 1. Vehicle hybrid propulsion system (bottom) with onboard fuel reforming (top).

The battery of the hybrid system can be used as an energy source for cold start; SRM is less sensitive to coke formation than methanol decomposition; and the DI method can allow increase in the ICE maximum power output and deal with pre-ignition problems. In a further investigation [13] they performed simulation and performance comparison of an ICE fed with different reforming products. The reforming products compositions used in [13] were derived from equilibrium calculations that were empirically corrected in case of methanol steam reforming. No assessments were made about availability of the energy required to sustain the considered reforming processes. It is clear that the engine performance is affected by the composition of the reforming products and the reforming products are affected by the exhaust gas temperature, composition and flow rate. Due to the tight interrelations between the two main parts of the considered ICE-reformer system, it is desirable to create a single model that simulates their joint operation.

Such a model can be used for determining the required properties of the reformer and its design. It can provide a tool for optimizing the design and operation parameters of the ICE-reformer system. Further on, this model can be applied to shed a light on the complicated transient behavior of the system. The importance of the model is that it provides a rather simplified way of exploring any ICE-reformer system by using the GT-Power software, and thus can help other research groups working on other TCR schemes.

In the current work the GT-Power based ICE model described in [13] is applied to simulate joint operation of direct-injection ICE with SRM reactor. It was applied to provide preliminary considerations on design requirement for the reformer.

STEAM TO METHANOL RATIO SETUP

There is a general consensus that the most active and selective catalysts for the endothermic SRM reaction are CuO/ZnO/Al_2O_3 based catalysts [14], hence the same type of catalyst was chosen for our simulations. The steam to methanol (or S/M) molar ratio in the reformer feed is an important parameter for its operation. Specifically, S/M ratios lower than 1 can provoke coke formation and deactivation of the catalyst and may also result in slower reaction rates. Due to these problems, most of the SRM research is focused on S/M ratios greater than 1 and we have used this limit in our work, as well. Choi and Stenger [15] found that at S/M ratios higher than 0.76 the products of SRM can considered to be limited to CO, CO_2, H_2O and H_2. For a given reformer size, the highest possible methanol conversion is an important condition for achievement of better efficiency and emissions reduction benefits. Thus, reforming conditions enabling maximal methanol conversion should be realized. Taking this into account, the following overall reforming reaction is preferred:

$$CH_3OH + y \cdot H_2O \rightarrow$$
$$x \cdot CO + (1-x) \cdot CO_2 + (y+x-1) \cdot H_2O + (3-x)H_2$$
$$\{0 \le x \le 1,\ 0 \le (y+x-1)\} \qquad (1)$$

where *x* is often referred to as CO selectivity factor [16].

This equation shows that the only factor affecting the lower heating value (LHV) of the reforming products is *x* and that the LHV of the mixture is rising linearly along with *x*. Higher S/M ratios lead to decrease of CO formation [17] and hence reduce the heating value of the SRM products. Furthermore the heat required for the evaporation of the added water will demand a larger heat transfer area between the exhaust gases and the fuel mixture at the evaporator. Agarwal [18] suggest that increasing S/M to 1.4 might increase the SRM reaction rate, thus enabling to downsize the reformer, but experiments made by Santacesaria [19] agree with his findings only at low temperatures (lower than 180 °C). Observations made by Lee et al [20] totally contradict these findings. Taking this information into account, it seems that for an ICE-SRM system the preferable S/M ratio should lie between 1 and 1.4. All the simulation results presented in this work were performed for S/M ratio of 1.

REFORMER MODELING

The GT-Suite package provides tools for modeling heat exchangers and chemical reactions. Chemical reactions are modeled through the use of “Global-Reactions” template and are usually used to simulate chemical reactions in the exhaust aftertreatment systems. There are also few options of heat

exchanger modeling. However, the "Global-Reactions" template cannot be used within one of the heat exchanger templates and GT-Suite does not have a built-in template for modeling a heat exchanger-reactor. Although GT-Power can cooperate with other modeling applications, it is clear that a solution within the program is superior in terms of computation time, model complexity and flexibility. Therefore, it was decided to develop a physical model that can be applied within the GT- Power software.

Physical Model

A 1-D homogeneous reformer model (i.e., ignoring interphase and intraphase concentration and temperature gradients) of a packed bed reactor (PBR) is considered. This type of reactor is very common for SRM, and enables changing the catalyst type and pellets size. Also, radial gradients are assumed to be negligible [21]. Moreover, combining the solid and gas phases into a pseudo-homogenous medium model makes possible a reasonable approximation of both flow and heat equations under low Mach and Reynolds numbers [22, 23, 24, 25]. It is not yet clear whether the total SRM reaction is better described by methanol decomposition ($CH_3OH \rightarrow CO+2\cdot H_2$) followed by water gas shift (WGS) ($H_2O+CO \rightarrow CO_2+H_2$) [14] or by direct SRM followed by reverse WGS (r-WGS) [16, 17]. If an empiric power law rate equation is used instead of a full kinetic derived schemes, either of the proposed paths can be chosen since they are linearly dependent. This approach leads to a set of 4 equations derived from the mass and energy conservation laws.

Mass conservation equations:

$$A_t \cdot \varepsilon \cdot \frac{\partial C_{CH_3OH}}{\partial t} = -\frac{\partial F_{CH_3OH}}{\partial z} - A_t \cdot \varepsilon \cdot r_1 \cdot \rho_{cat} \tag{2}$$

$$A_t \cdot \varepsilon \cdot \frac{\partial C_{CO_2}}{\partial t} = -\frac{\partial F_{CO_2}}{\partial z} + A_t \cdot \varepsilon \cdot (r_1 - r_2)\rho_{cat} \tag{3}$$

Energy conservation equations for counter current flow:

$$A_t \cdot \rho_{eff} \cdot Cp_{eff} \cdot \frac{\partial T_{eff}}{\partial t} = \left(-\frac{\partial \left((\sum_{i=1}^{5} Cp_i \cdot F_i) T_m \right)}{\partial z} + A_t \cdot k_{eff} \frac{\partial^2 T_{eff}}{\partial^2 z} + A_t \cdot (\Delta H_1 \cdot r_1 + \Delta H_2 \cdot r_2)\rho_{cat} + U \cdot P \cdot (T_{exh} - T_{eff}) \right) \tag{4}$$

$$A_S \cdot \rho_{exh} \cdot Cp_{exh} \cdot \frac{\partial T_{exh}}{\partial t} = \left(-\frac{\partial (Cp_{exh} \cdot F_{exh} \cdot T_{exh})}{\partial z} + A_S \cdot k_{exh} \frac{\partial^2 T_{exh}}{\partial z^2} - U \cdot P \cdot (T_{exh} - T_{eff}) \right) \tag{5}$$

Where:

C_i-Molar density of species i; F_i -Molar flow rate of species i; A_t -Cross sectional area of the PBR; ε -Porosity of the PBR; ρ_i -Density of species i; Cp_i -Constant pressure molar heat capacity of species i; A_s -Cross sectional area of the exhaust gas flow; U -Overall heat transfer coefficient; P -Wetted perimeter between exhaust gas and reforming products; T_i - Temperature of species i; k_i -Heat conductance of species i; z -Length coordinate along the PBR axis; r_1 -SRM reaction rate per unit of catalyst load. r_2 -RWGS reaction rate per unit of catalyst load; ΔH_1 -SRM heat of reaction; ΔH_2 -RWGS heat of reaction. Subscript: *eff* -Effective property of the pseudo-homogenous medium; *exh* -Exhaust gases; *cat* -Catalyst;

The boundary conditions are the properties of the exhaust gas and the evaporated water-methanol mixture at the entrance to the reformer.

Reaction Kinetics

Many reaction rate expressions have been proposed for r_1 and r_2. Each of them was derived from a different experimental setup, operating conditions and catalyst types. In some of the provided reaction rates, diffusion limitations are already incorporated, in some effectiveness factor should be applied and others use temperature related polynomial to extend the limits of their expressions. Therefore, it is critical to be careful in choosing the right reaction rate and, if possible, to make experiments and derive relevant and more accurate rate expressions. Empirical reaction rate is usually the Arrhenius type expression of the form:

$$r = k_1 \cdot f_1(T,P) \cdot \exp\left(\frac{-E_{a,1}}{R \cdot T}\right) \cdot \prod P_i^{S_{1,i}} - k_{-1} \cdot f_{-1}(T,P) \cdot \exp\left(\frac{-E_{a,-1}}{R \cdot T}\right) \cdot \prod P_i^{S_{-1,i}} \tag{6}$$

k_i -Pre-exponential rate constant; E_a -Activation energy; R - Universal gas constant; T -Temperature; P_i -Partial pressure of species i; S_i -The reaction order related to species i;

We incorporate two reactions: the practically irreversible SRM (at 1 bar) and the reversible r-WGS. The SRM is described by the power law reaction rate expression based on Purnama's [16] for a $CuO/ZnO/Al_2O_3$ catalyst, in temperatures above 230 °C:

$$r_1 = 1.95 \cdot 10^5 \cdot \exp\left(\frac{-76[kJ/mol]}{R \cdot T}\right) P_{H_2O}^{0.4} \cdot P_{CH_3OH}^{0.6} \left[\frac{mol}{s \cdot g_{cat}}\right] \tag{7}$$

and the correlation derived by Lee et al. [20] for a CuO/ZnO/Al_2O_3 catalyst for temperatures below 230 °C:

$$r_1 = 2.19 \cdot 10^6 \cdot \exp\left(\frac{-103[kJ/mol]}{R \cdot T}\right) \cdot P_{CH_3OH}^{0.564} \cdot (P_{H_2} + 11.6[kPa])^{-0.647} \left[\frac{mol}{s \cdot g_{cat}}\right] \quad (8)$$

The r-WGS reaction for the entire temperature range was taken from [16] to be:

$$r_2 = 3.1 \cdot 10^6 \cdot \exp\left(\frac{-108[kJ/mol]}{R \cdot T}\right) \cdot P_{CO2} \cdot P_{H_2} - 2.5 \cdot 10^4 \cdot \exp\left(\frac{-67[kJ/mol]}{R \cdot T}\right) \cdot P_{H_2O} \cdot P_{CO} \left[\frac{mol}{s \cdot g_{cat}}\right] \quad (9)$$

Heat Transfer

The heat transfer coefficient from the exhaust gas side was calculated using a concentric tube annulus correlation from [26] for the ratio of the selected heat exchanger's diameters:

$$Nu_i(D_i / D_o = 0.69) \cong 5.4 \quad (10)$$

Where: D_i -Inner diameter of the annulus tube; D_o -Outer diameter of the annulus tube.

Srinivasan [21] uses the following correlation to calculate the heat transfer coefficient between the PBR and the ambient surroundings:

$$h_\infty = \frac{4 \cdot k_\infty \cdot \left(0.2 \Pr^{1/3} \cdot \left(\frac{\rho_s \cdot u_s \cdot d_p}{\mu_s}\right)^{0.8}\right)}{D} \quad (11)$$

Where: ρ_s -density of the reformate; Pr -Prandtl number of the reformate; u_s -velocity of the reformate; μ_s -the dynamic viscosity of the reformate; k_∞ -heat conductance of the surroundings;

This correlation is valid for $Bi_\infty = \frac{h_\infty \cdot D}{4 \cdot k_{eff}} < 1$.

After comparing 20 different ways for calculating k_{eff}, Srinivasan [21] reported that the equation:

$$k_{eff} = k_s^{\varepsilon} \cdot k_{cat}^{1-\varepsilon} \quad (12)$$

developed by Neild and Bejan [22] provides good results.

To evaluate k_{eff}, it is necessary to know the porosity. We applied the approach of Ribiero [27] for porosity calculation and used the expression:

$$\varepsilon = 0.373 + 0.914 \cdot \exp(-0.824 \cdot D / d_p) \quad (13)$$

Where: D -Internal PBR diameter; d_p -Diameter of the catalyst pellets. Equation (13) is valid for $19 > D/d_p > 2$.

The heat transfer resistance of the PBR tube wall is small relative to that between the reactor wall and the surrounding fluids on both his sides and hence can be neglected. Equations (10, 11, 12, 13) were applied to account for the heat transfer process in the reformer.

Implementation into GT-Power

For simplicity an example of a counter-current tube-in-tube heat exchanger-reactor contained of 100 tubes was created. Figure 2 shows an example of a small scale reformer model as it was built in the GT-Power. The reformer is divided to a number of mixed sections. Each section has uniform fluid properties. Eq. (7, 8, 9) are inserted to the reforming model ("Reforming_Reactions" object). The objects that describe the convection between the exhaust gas and the heat exchanger's wall (objects "h-a" up to "h-c") are set through eq. (10). The objects describing the convection between the wall and the reformate gas ("h1-h3") are calculated with eq. (11). A large value was assigned for the heat transfer coefficient between the exhaust gas and the pellets (to obtain a homogenous model ("Pellets_To_Reformate_Convection" objects)). The conductivity along the reformer axis ("Effective_Conductance" object) is calculated with eq. (12).

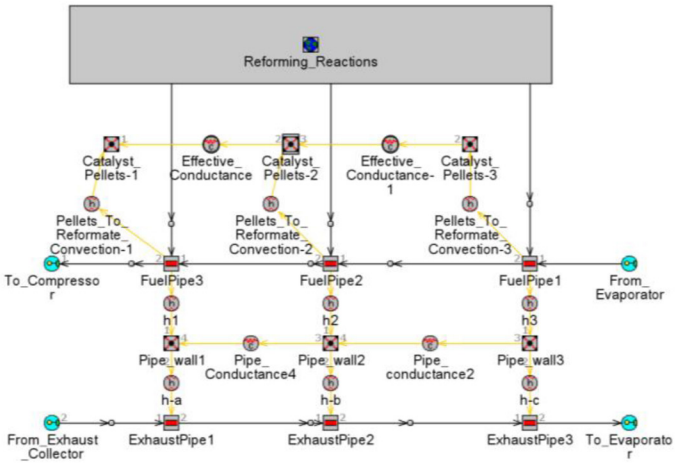

Figure 2. A scheme of a small scale reformer.

The internal diameter of the inner and outer tubes was set to 10 mm and 16 mm accordingly. Thus, the reformer length remained as the only undetermined parameter left for setting the overall heat transfer area. To allow a heat exchanger-reactor modeling inside the GT-Power package, an approach of dividing the reformer to zero-dimension segments was applied. In each segment the mass, energy and momentum conservation equations were solved. The division to segments was made by meeting a demand for average temperature difference of no more than 10°C between two consecutive

segments in which reaction occurs. This was done to reduce the error resulting from the temperature spatial averaging, since the reaction rate is exponentially dependent on the temperature. The chemical reactions were considered through the "Global-Reactions" template. Since the chemical scheme contains reactions with considerably different reaction rates, then the set of equations forms a stiff ODE system. The robust RADAU method was used for the numeric solution of these equations, as recommended in [28].

Model Validation

The newly developed reformer model was validated using available experimental data of a small scale isothermal reactor. The experimental results reported by Purnama [16] were a good source of comparison since they were obtained for the reformer similar to the one considered in our example-Table 1.

Table 1. Selected experiment parameters from Purnama [16].

Pellets size (d_p)	$0.71-1[mm]$
Internal PBR diameter (D)	$10[mm]$
Steam-to-methanol ratio, (S/M)	1
Catalyst load-to-flow rate ratio, (W/F_m)	$2-20\left[g_{cat}\cdot s/mmol\right]$
Temperature range (T)	$230-300[^oC]$
Pressure (P)	$1[atm]$

For TCR applications with SRM the accurate prediction of methanol conversion is of high importance because of its significant effect on engine performance and pollutants formation. Thus, model validation by comparison of the predicted and experimentally measured methanol conversion fractions was carried out. Simulation results for different temperatures and W/F_m ratios were compared to the experimental fitted curves presented by Purnama in the conversion range of 45%-100%. The comparison results are shown in Figure 3.

As can be seen from Figure 3, the model provides an acceptable agreement with experimental data - maximal error does not exceed 20%. The simulation gives better fit to the experimental results in the mid of the temperature range and at high conversion. At the temperatures relevant for our application a difference between the predicted and measured results is usually less than 5%.

Most of the data presented by Purnama [16] is in the area of incomplete conversion, where the CO levels did not exceed 2.5%. In case of incomplete conversion, CO selectivity factor (x in eq. 1) is very low and the reformate is mainly composed from hydrogen and carbon dioxide, in addition of the unreformed methanol and water. Our predictions for the same conditions as in Purnama's experiments provide CO levels exactly in the same range.

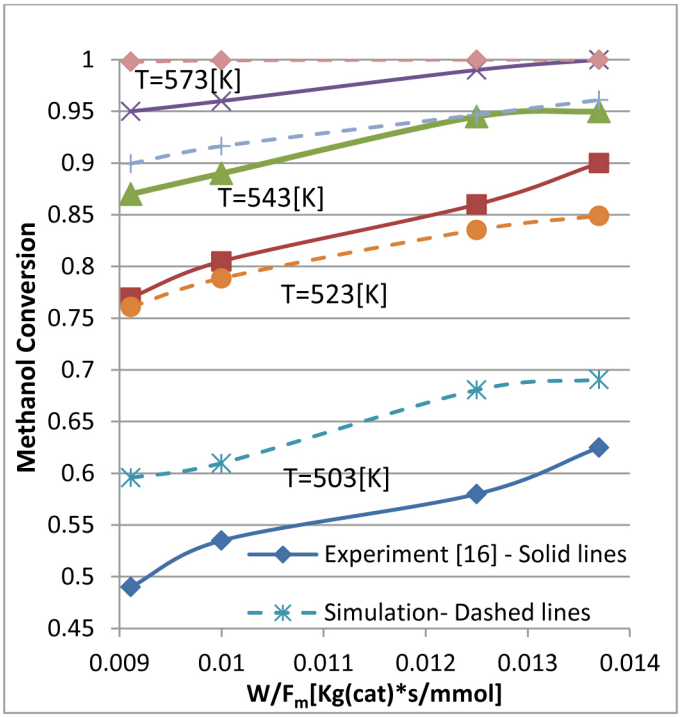

Figure 3. Comparison of predicted and experimentally obtained methanol conversion at different temperatures and flow rates.

SI ENGINE MODELING

The applied engine model is described in detail in [12, 13]. Since there is no available experimental data that suggest numeric values of the coefficients in the Wiebe model adjusted to the gaseous fuel compositions considered in the current work, an approach suggested in [28] was applied. Anchor angle (corresponds to 50% of fuel burned) and combustion duration of 10% - 90% fuel were used as variable inputs for Wiebe model, governing heat release rate as a function of a crank angle. Actual burning velocities of the considered fuels inside a cylinder were assumed to be proportional to the appropriate laminar flame velocities (taking into account that the engine geometry and operation regime remained the same with change of the fuel type). Laminar flame velocity for each of the considered gaseous fuel compositions was estimated through interpolation with a GT-Power 'LookUp' multidimensional map. The map was built based on the published experimental data from [29, 30, 31] and is presented in Table 2.

For the flame speed calculation the methanol vapors were assumed to behave as CO, since they have approximately the same laminar flame speed. The water and CO_2 absorb heat from the combustion thus decreasing the flame speed. Their molar heat capacity is of the same order of magnitude, so water percentage was added to that of the CO_2. Since the molar fractions of water and methanol are small, the error resulting from the assumptions mentioned above should be small as well. Woschni correlation for an engine without swirl was used for calculation of the in-cylinder heat transfer, as described in [32]. Energy required for cooling, compression

and injection of gaseous reforming products into the engine cylinder was not assessed. The main parameters of the direct injection, naturally aspirated SI engine that was used as an example to demonstrate capabilities of the developed model are listed in Table 3.

Table 2. Laminar flame speed as a function of Lambda and CO-H_2-CO_2 mixture composition at normal conditions [29, 30, 31].

Lambda	% mol H2	% mol CO	% mol CO2	Laminar flame speed[cm/s]
1.09	95	5	0	195
1.32	95	5	0	130
1.36	95	5	0	122
1.49	95	5	0	99
1.61	95	5	0	84
1.67	95	5	0	80
0.98	76	4	20	152
1.05	76	4	20	142
1.25	76	4	20	105
1.32	76	4	20	93
1.39	76	4	20	85
1.57	76	4	20	65
1.63	76	4	20	60
1.00	73	0	27	133
1.00	54	0	46	75
1.00	50	50	0	113
1.10	50	50	0	98
1.21	50	50	0	82
1.36	50	50	0	66
1.49	50	50	0	52
1.56	50	50	0	47
1.65	50	50	0	43
1.00	41	0	59	42
0.99	40	40	20	85
1.08	40	40	20	76
1.19	40	40	20	65
1.32	40	40	20	55
1.48	40	40	20	44
1.61	40	40	20	38
1.00	31	0	69	20
0.94	5	95	0	42
1.50	5	95	0	22
0.98	4.5	85.5	10	34
1.43	4.5	85.5	10	21
1.33	100	0	0	135
2	100	0	0	50

Table 3. Main parameters of the simulated engine.

Cylinder Bore	90 mm
Piston Stroke	90 mm
Number of Cylinders	4
Compression ratio	10:1
Rated Speed	4000 rpm
Rated Brake Power	75 kW
BMEP	9.8 bar

POSSIBLE MODEL APPLICATIONS

Analysis and Optimization of ICE-SRM Design

The strength of the ICE-SRM joint model is best demonstrated by showing the combined effects of reformer design and engine operation parameters on the performance of the whole ICE-SRM system. This is shown in Figures 4, 5, 6, 7.

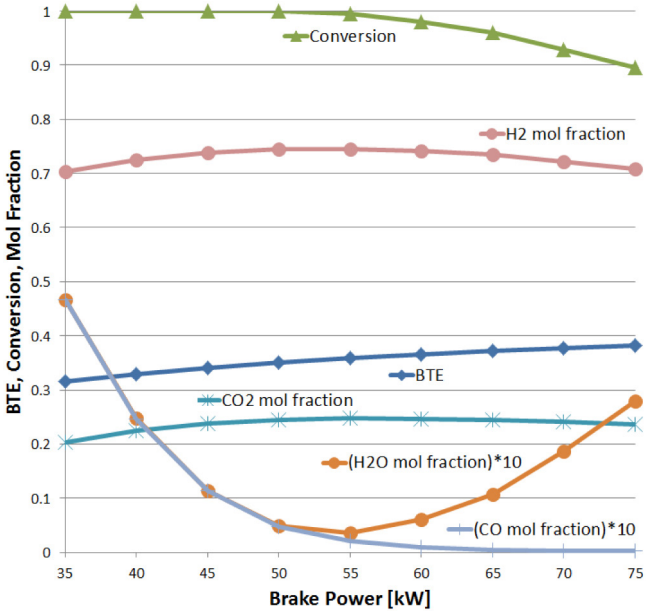

Figure 4. BTE, Conversion and reforming gas molar fractions Vs brake power. Speed=4000 rpm, λ=1.3, Reformer heat transfer area =1.06 m^2.

As can be seen from Fig. 4, for the given reformer size methanol conversion drops as power exceeds 55 kW. As the brake power grows, there is a higher fuel flow through the reformer (lower W/F_m). Thus the reformer does not provide full conversion. At lower power the CO content in the reforming products is higher due to the reduced fuel flow. Even though the fuel's LHV for the given reformer reaches a maximum at the lowest power (highest CO selectivity), the best BTE is achieved at high power. This is a result of the reduced pumping work at wider throttle opening, which has a greater impact on the BTE than the small change in the LHV.

Figure 5 demonstrates the effect of the reformer length and ignition timing on methanol conversion. Retarded spark timing results in higher exhaust gas temperatures that enhance methanol conversion. This is an additional proof of the need to consider and analyze the ICE-SRM system as a whole.

For the considered example, in the region of $1<\lambda<1.3$ the engine brake power was maintained constant at 75 kW by controlling the throttle. Since at $\lambda \approx 1.3$ the throttle was already wide-open, Lambda values higher than 1.3 could not be realized by changing the amount of air induced into the cylinder. Thus, they were set by reducing the amount of reformate injected to the cylinders. In the constant power

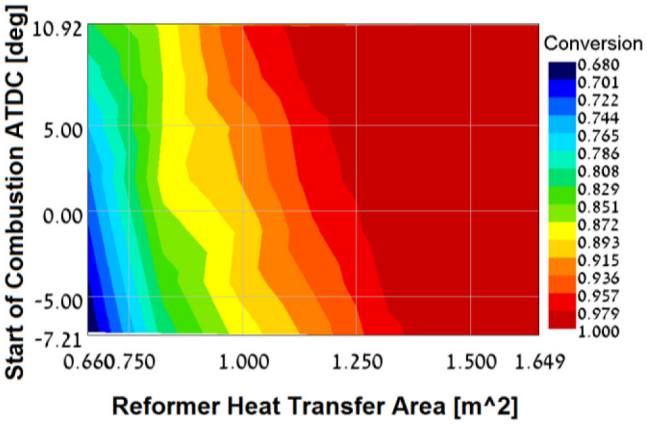

Figure 5. The effect of reformer length and ignition timing on methanol conversion. P=75 kW, n=4000 rpm, λ=1.3.

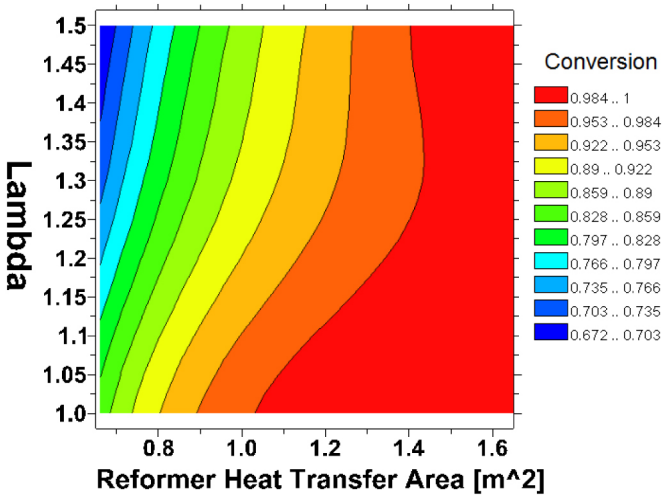

Figure 6. Methanol conversion vs. lambda and reformer heat transfer area. Power = 75 kW (Up to λ=1.3, for λ>1.3 WOT), speed = 4000 rpm.

region of figure 6 (i.e. 1<λ<1.3) the conversion decreases with Lambda increase. This happens because higher Lambda values lead to reduction of the exhaust gas temperature and thereby - to lower heat transfer rate between the exhaust and the reforming gases. The inadequate heat transfer results in incomplete methanol conversion. In the area of λ>1.3 an oppositely influencing factor comes into effect. The reduced fuel flow rate increases the W/F_m ratio and the residence time of the reacting gases in the reformer and consequently the reforming temperature. The influence of the fuel flow rate can be seen in the gradient change of the constant conversion lines around λ=1.3. From the analysis example shown in Fig 6, it can also be deduced that if full methanol conversion is a prerequisite and the engine is intended to work lean-burn with λ>1.3, then a 1.5 m^2 reformer is required. For engine operation regimes with λ<1.1, when methanol conversion of 95% is acceptable, the reformer heat transfer area of 1 m^2 will be adequate. In the simulations of the proposed reformer the average overall heat transfer coefficient was $U = 30 - 40\left[\frac{W}{m^2 \cdot K}\right]$. Obviously, an increase in the heat transfer coefficient that may be achieved through advanced heat exchanger design will lead to a reduction of the reformer size.

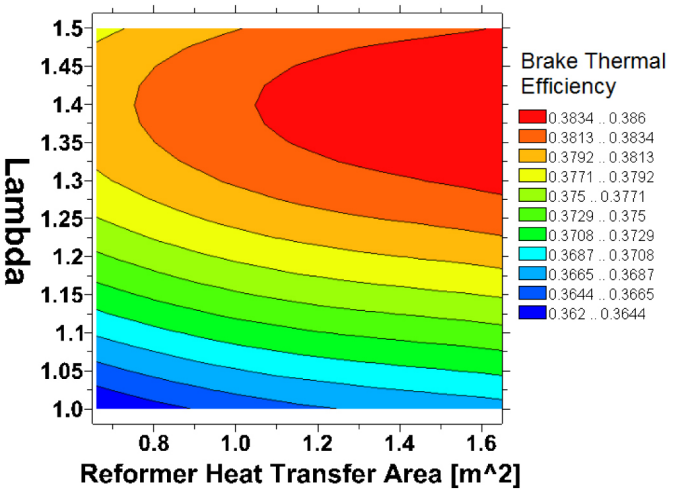

Figure 7. Brake thermal efficiency of the ICE-SRM system vs. lambda and reformer heat transfer area. Power = 75 kW (Up to Lambda=1.3, for Lambda>1.3 WOT), speed = 4000 rpm.

As expected, the engine's BTE increases together with a rise in the reformer's heat transfer area (Fig. 7). This is due to the higher LHV of the reforming products in the bigger reformer. It can also be noticed that the lean operation has higher contribution to the BTE improvement than the increase of the fuel LHV (the gradient along Lambda higher than the gradient along heat transfer area). This finding is in a good agreement with data reported by Brinkman and Stebar [6]. Despite the anticipated fact that a bigger reformer is always advantageous at the given operation conditions (in terms of BTE), the reformer's size should be one of the optimization parameters together with engine geometry and its tuning data. Considering reformer size will make possible including additional important parameters, as weight and manufacturing costs, into the process of system design optimization. If one would like to avoid aldehydes formation and corrosion problems related with the methanol presence in the cylinder, the reformer should provide full methanol conversion at all operation modes. This could be achieved by an appropriate design of a reformer based on the results of modeling and analysis of the whole ICE-SRM system. Enlargement of the reformer beyond the size that ensures full conversion, in order to increase the LHV, probably wouldn't be cost-effective.

Transient Event Simulation

As an example, a case of linear load increase from 30 to 60 kW within 2 sec was examined under constant speed of 4000 rpm and λ=1.3. The model was first run in the low power regime until it reached steady state. Then the throttle controller was set to increase the load linearly within 2 sec. This was realized through a PID controller that operated the throttle

causing a slight over shoot in power before reaching the steady state. The variation of several selected parameters during the transient event is plotted in Figure 8.

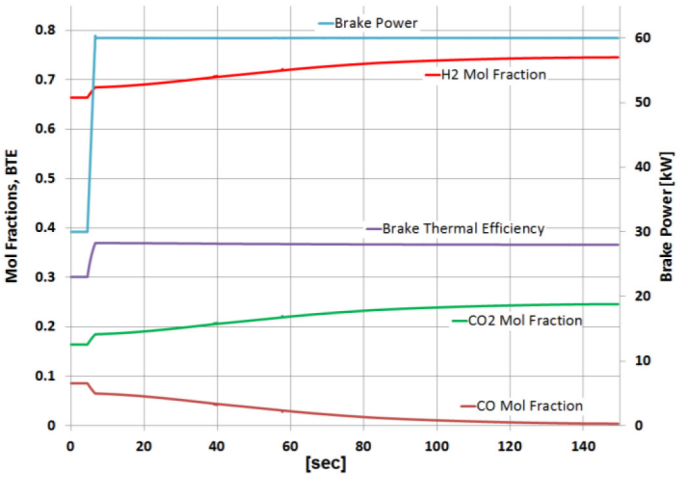

Figure 8. Transient event in the ICE-SRM system. Response of the power, efficiency and molar fractions of the reforming products to a linear target change in brake power. Speed = 4000 rpm, λ=1.3, Reformer heat transfer area =1.06 m^2.

Prediction results show that at the low power regime CO levels are high due to the reduced fuel flow and elevated temperatures of the reformer. As power starts to rise, the fuel flow rate is increased causing a sharp change in the molar fractions of the reformate gas. After the power has reached 60 kW the fuel flow rate is remained almost constant (slight increase due to small decrease in BTE). At this stage the change in molar fractions of the reforming products is caused by the temperature decrease of the reformer. Since the thermal response is slow, a long time is required for the engine fuel (SRM products) to reach its steady state composition (in this case 140-150 sec). This phenomenon has to be taken into account when developing the ICE-SRM system. Reformer design parameters such as catalyst type and load would have an effect on the system's transient response properties. The observed BTE increase is a result of the reduced pumping work. At about 7 sec after the start of the transient event, when the pumping work is already reduced, but the CO levels are still higher than at steady state, the BTE reaches maximum value. After that, it is gradually dropping as the CO content in the reforming products declines.

FURTHER RESEARCH

The authors would like to stress the fact that optimization of the engine design and operating parameters has not been performed yet and is planned as a further research. The directions of future research will include optimization of the heat-exchange process in the reformer, increasing the catalyst load, reducing pellets size to enhance the reaction rates and verifying simulation results through experiments. A detailed study of transient processes in the ICE-SRM system is planned to be performed by using the developed simulation tool.

SUMMARY

This paper describes the model for simulation of the joint operation of internal combustion engine with methanol steam reformer. We tried to emphasize a need for such a model and outline some opportunities derived from its creation. The most important of them are: a possibility to perform a comprehensive analysis and design optimization of the whole ICE-SRM system and an opportunity to study and understand processes inside this complex system during various transient events.

The developed model was applied for a simulation of an ICE-SRM system. The obtained preliminary results allow us to derive some important observations. As expected, the engine's BTE increases together with a rise in the reformer's heat transfer area. This is due to the higher LHV of the reforming products in the bigger reformer. However, the lean operation, that was possible because of the hydrogen-rich reformate fuel, has higher contribution to the BTE improvement than the increase of the fuel's LHV.

Performed calculation showed that at WOT influence of lambda increase has a complex behavior. On the one hand, higher Lambda values lead to reduction of the exhaust gas temperature and thereby - to lower heat transfer rate between the exhaust and the reforming gases, which tends to reduce conversion. On the other hand, the reduced fuel flow rate increases the W/F_m ratio and the residence time of the reacting gases in the reformer and consequently - the reforming temperature, which tends to increase conversion.

First simulations of a transient event using the developed model show that with a power rise, the fuel flow rate is increased causing a sharp change in the molar fractions of the reformate gas. After the power has reached the target value, the fuel flow rate is remained almost constant. At this stage a slower change in the molar fractions of the reforming products is observed. It is caused by the temperature change of the reformer.

REFERENCES

1. International Energy Agency, World energy outlook 2011. OECD/ IEA, Paris, France, 9 November 2011
2. Chakravarthy VK, Daw CS, Pihl JA., Conklin JC. “Study of the Theoretical Potential of Thermochemical Exhaust Heat Recuperation for Internal Combustion Engines.” *Energy Fuels*, 2010: 1529-1537.
3. Petterson, L. Sjostrom, K. “Decomposed Methanol as a Fuel-A review.” *Combust, Sci. and Tech.*, 1991: 265-303.
4. Finegold, Joseph G. “Dissociated Methanol Vehicle Test Results.” Inst of Gas Technology, 1984.
5. Sakai, T., Yamaguchi, I., Asano, M., Ayusawa, T. et al., “Transient Performance Development on Dissociated Methanol Fueled Passenger Car,” 1987.
6. Brinkman, N. and Stebar, R., “A Comparison of Methanol and Dissociated Methanol Illustrating Effects of Fuel Properties on Engine Efficiency-Experiments and Thermodynamic Analyses,” SAE Technical Paper 850217, 1985, doi:10.4271/850217.
7. Morgenstern D.A., Fornango J.P, “Low-Temperature Reforming of Ethanol over Copper-Plated Raney Nickel: A New Route to Sustainable Hydrogen for Transportation,” Energy and Fuels, vo. 19, (2005), 1708-16

8. Morgenstern, D., Wheeler, J., and Stein, R., "High Efficiency, Low Feedgas NOx, and Improved Cold Start Enabled by Low-Temperature Ethanol Reforming," *SAE Int. J. Engines* 3(1):529-545, 2010, doi:10.4271/2010-01-0621.
9. Sall, E.D. Morgenstern, D.A. Fornango, J.P. Taylor, J.W. et al. "Reforming of Ethanol with Exhaust Heat at Automotive Scale" *Energy & Fuels* 2013 27 (9), 5579-5588
10. Hoffmann, W., Wong, V., Cheng, W., and Morgenstern, D., "A New Approach to Ethanol Utilization: High Efficiency and Low NOx in an Engine Operating on Simulated Reformed Ethanol," SAE Technical Paper 2008-01-2415, 2008, doi:10.4271/2008-01-2415.
11. Tartakovsky, L., Mosyak, A. and Zvirin, Y., "Energy analysis of ethanol steam reforming for internal combustion engine", Int. J. Energy Research 37: 259-267, 2013, doi:10.1002/er.1908.
12. Tartakovsky, L., Baibikov, V., Gutman, M., Mosyak, A. et al., "Performance Analysis of SI Engine Fueled by Ethanol Steam Reforming Products," SAE Technical Paper 2011-01-1992, 2011, doi:10.4271/2011-01-1992.
13. Tartakovsky, L., Baibikov, V., and Veinblat, M., "Comparative Performance Analysis of SI Engine Fed by Ethanol and Methanol Reforming Products," SAE Technical Paper 2013-01-2617, 2013, doi:10.4271/2013-01-2617.
14. Tesser, R. Di Serio, M. and Santacesaria, E. "Methanol steam reforming: A comparison of different kinetics in the simulation of a packed bed reactor," Chem. Eng. J. 154(1-3):69-75, 2009.
15. Choi, Y. Stenger, H.G. Appl. Catal. B 38 (2002) 259.
16. Purnama, H., Ressler T., Jentoft R. E., Soerijanto H., Schlogl R., and Schomacker R. "CO formation/selectivity for Steam Reforming of Methanol with a Commercial CuO/ZnO/Al2O3 Catalyst." Applied Catalysis A: General 259, no. 1 (2004): 83-94.
17. Agrell, J. Birgersson, H. Boutonnet, M. "Steam Reforming of Methanol Over a Cu/ZnO/Al2O3 Catalyst: A Kinetic Analysis and Strategies for Suppression of CO Formation." Elsevier, 2002.
18. Agarwal, V. Patel, S.; Pant, K. K. "H2 production by steam reforming of methanol over Cu/ZnO/Al2O3 catalysts: transient deactivation kinetics modeling", Appl. Catalysis. A. 2005, 155, 279
19. Santacesaria, E. Carrá, S., "Kinetics of catalytic steam reforming of methanol in a cstr reactor," Applied Catalysis 5(3):345-358, 1983.
20. Lee, J.K. Ko, J.B. Kim, D.H. "Methanol steam reforming over Cu/ZnO/Al2O3 catalyst: kinetics and effectiveness factor." *Applied Catalysis* 278 (2004): 25-35
21. Srinivasan A. and Depcik C., "One-Dimensional Pseudo-Homogeneous Packed-Bed Reactor Modeling: I. Chemical Species Equation and Effective Diffusivity," Chem. Eng. Technol. 36(1):22-32, 2013.
22. Wakao, N. Kaguei, S. "Heat and Mass Transfer in Packed Beds", Topics in Chemical Engineering, Vol. 1, Taylor & Francis, New York 1982.
23. Nield, D.A. Bejan, A. Convection in Porous Media, 3rd ed., Springer-Verlag, New York 2006.
24. Younis, L. J. Inst. Energy 2006, 79 (4), 222-227 DOI:10.1179/174602206X148874
25. Finlayson, B. A. Chem. Eng. Sci. 1971, 26 (7), 1081-1091. DOI:10.1016/0009-2509(71)80022-2
26. Rosenhow, W.M. and Hertnett, J.P. *handbook of heat transfer*. New York: McGraw-Hill, 1972.
27. Ribeiro, A.M. Neto, P. and Pinho, C., "Mean Porosity and Pressure Drop Measurements In Packed Beds Of Monosized Spheres : Side Wall Effects", International Review of Chemical Engineering, Vol. 2, No. 1, PP. 40-46, 2010.
28. GT-Power Engine Simulation Software, Gamma Technologies, Inc.
29. Natarajan, J., Lieuwen, T. and Seitzman, J., "Laminar flame speeds of H2/CO mixtures: effect of CO2 dilution, preheat temperature and pressure", Combustion & Flame, 151: 104-119, 2007.
30. Qiao, L. Kim, C.H. Faeth, G.M. "Suppression effects of diluents on laminar premixed hydrogen/oxygen/nitrogen flames"
31. Aung, K. T. Hassan, M. I. Faeth, G. M. "Flame Stretch Interactions of Laminar Premixed Hydrogen/Air Flames at Normal Temperature and Pressure"
32. Heywood, J.B., "Internal combustion engines fundamentals", New York, McGraw-Hill, 1988.

CONTACT INFORMATION

Arnon Poran
The Nancy and Stephen Grand Technion Energy Program
Technion- Israel Institute of technology
+ 972-544-261-177
arnonp@tx.technion.ac.il

Leonid M. Tartakovsky
+972-4-8292077
tartak@technion.ac.il

ACKNOWLEDGMENTS

The financial support of the Israel Science Foundation is highly appreciated. The authors acknowledge the support from the Nancy and Stephen Grand Technion Energy Program (GTEP). We sincerely thank to Mr. Mike Arnett and Mr. Ryan Dudgeon from GTI support group for their help and cooperation.

DEFINITIONS/ABBREVIATIONS

BMEP - brake mean effective pressure

BTE - brake thermal efficiency

CA - crank angle

CD - combustion duration

DI - direct injection

ICE - internal combustion engine

ID - inner diameter

LHV - lower heating value

ODE - ordinary differential equation

PBR - packed bed reactor

r-WGS - reverse water gas shift

SI - spark ignition

SRE - steam reforming of ethanol

SRM - steam reforming of methanol

S/M - steam to methanol molar ratio

TCR - thermo-chemical recuperation

TDC - top dead center

WGS - water gas shift

WOT - wide open throttle

W/F_m - catalyst load to initial methanol flow rate ratio